Ferroelectric mode and molecular structure in the hydrogen-bonded ferroelectric arsenates and their deuterated isomorphs*

R. P. Lowndes, N. E. Tornberg, and R. C. Leung
High Pressure Physics Laboratory, Northeastern University, Boston, Massachusetts 02115
(Received 17 August 1973; revised manuscript received 4 February 1974)

Light-scattering measurements of the temperature dependence of the Raman-active modes of vibration in both the paraelectric and ferroelectric states of the hydrogen-bonded ferroelectrics KH_2AsO_4, RbH_2AsO_4, and CsH_2AsO_4 and their deuterated isomorphs KD_2AsO_4, RbD_2AsO_4, and CsD_2AsO_4 are reported. Through examination of these spectra we have identified the protonic or deuteronic, transverse-optic, AsO_4^{3-} internal, and O–H–O or O–D–O valence vibrations in the Raman scattering and determined their symmetries and temperature dependence. Evidence for the collective protonic or deuteronic motions is observed in both the low-frequency B_2 and E spectra in the paraelectric phase of each arsenate. The low-frequency B_2 spectra for the hydrogenated compounds are well fitted by a coupled-oscillator system representing the ferroelectric mode and a low-frequency phonon. The low-frequency B_2 spectra for the deuterated materials reveals the ferroelectric mode to be coupled to at least two low-frequency phonons, but, in a limited way, the spectra can be fitted to a coupled-oscillator system representing the ferroelectric mode and the lowest B_2 phonon. The results reveal the T/τ for the ferroelectric mode of all the compounds to decrease linearly with decreasing temperature; for real coupling the T/τ extrapolate to zero well below the transition temperature but for imaginary coupling the T/τ vanish much closer to the transition. In the limit of small damping, the results for real coupling are found to be in only partial agreement with the Kobayashi model, while the results for imaginary coupling are in accord with the Cowley-Coombs anharmonic theory of the transition and reveal the anomalous self-energy to be small compared to the conventional anharmonic self-energy of the soft mode.

I. INTRODUCTION

Descriptions of the ferroelectric transition in hydrogen-bonded ferroelectrics, such as KH_2PO_4 (KDP), have generally invoked a cooperative ordering of protons in a double-well potential along each hydrogen bond. de Gennes[1] originally showed that the individual tunneling of protons between a double-minima potential well would lead to collective tunneling excitations in the presence of proton-proton interactions, and Brout *et al.*[2] and Tokunaga[3] showed that such collective tunneling excitations would have a soft-mode temperature dependence. Kobayashi[4] extended this concept to include a coupled interaction between a collective proton tunneling mode and a transverse-optic lattice vibration polarized along the c axis of the crystal and showed that one of the coupled modes, the ferroelectric mode, of such a system would have a soft-mode temperature dependence. Dvorák[5] has modified the Kobayashi theory by taking into account the interaction of the a-polarized transverse-acoustic phonon both with the proton tunneling mode and the transverse-optic phonon polarized along the c axis; in this theory, as the transition is approached in the paraelectric phase, the ferroelectric mode drives the acoustic mode toward zero frequency via the piezoelectric interaction.[6,7] Recently, there have appeared doubts in the literature[8–10] as to whether the proton-tunneling model, originally due to Blinc,[11] and its extensions[1–5,12] can give a unified description of the ferroelectric transition in hydrogen-bonded ferroelectrics. Blinc *et al.*[8] have pointed out that at high temperatures the approximation used by Kobayashi of linear equations of motion will break down leading to diffusional rather than oscillatory solutions. Reese *et al.*[10] have also commented on this and have further remarked that the use of the molecular-field approximation to describe the spontaneous polarization is unlikely to yield an accurate description of the temperature dependence of the ferroelectric mode in view of the failure of the molecular-field theory to predict the rather unusual thermodynamic properties of KDP. Very recently, a number of authors[13–16] have attempted to discuss the ferroelectric transition in hydrogen-bonded ferroelectrics in terms of anharmonic phonons. In view of these different approaches and their associated theoretical difficulties, it is clear that studies of the line shape and temperature dependence of the ferroelectric mode on any relevant hydrogen-bonded ferroelectrics may help elucidate a more satisfactory description of the ferroelectric transition in these materials.

In this paper we report on light-scattering measurements of the Raman-active modes of vibration in both the paraelectric and ferroelectric states of the hydrogen-bonded ferroelectrics KH_2AsO_4 (KDA), RbH_2AsO_4 (RbDA), CsH_2AsO_4 (CsDA), and their deuterated isomorphs KD_2AsO_4 (KD*A), RbD_2AsO_4 (RbD*A), and CsD_2AsO_4 (CsD*A). Although the

ferroelectric-arsenate family is isomorphous with the ferroelectric-phosphate family, which is typified by KDP, relatively few spectroscopic investigations have been previously reported for the former family compared to the latter. The molecular spectra of KDA[17,18] have been reported and the low-frequency B_2 spectra associated with the ferroelectric mode have been investigated in KDA and CsDA[19] and, in a preliminary report of the present work, in RbDA.[20] In this paper we use our measurements to discuss the molecular structure of the arsenates above and below the ferroelectric transition and to investigate the nature of the mechanism responsible for this transition in the light of current theories. In a following paper we shall report on the influence of pressure on the Raman-active modes of vibration of these materials and its consequence for the molecular spectra and the ferroelectric mode.

II. EXPERIMENTAL

The Raman measurements were performed using excitation from a Coherent Radiation model 52G argon-ion laser providing about 800 mW at 514.5 nm. Using a right-angle scattering geometry, the scattered radiation was analyzed by a Spex 1401 dual spectrometer used in conjunction with a cooled ITT FW-130 photomultiplier and pulse-counting electronics. The Raman intensities were recorded on strip chart and, to facilitate the computer line-shape analyses discussed within the following text, were determined to an accuracy of better than ±1% using a traveling-microscope arrangement.

The Raman measurements were performed as a function of temperature in the range 5–350 K. The temperatures were achieved with an Air Products gas-transfer refrigerator using liquid helium as the gas source. The temperature stability for the duration of a recorded spectrum was better than ±1 K.

The samples used were oriented single crystals obtained from Gould Laboratories, Chicago, for the hydrogenated compounds and from Quantum Technology, Toronto, for the deuterated compounds, and were typically at least 7×7×4 mm in size. The deuterated samples were supplied with a 98% or better level of deuteration for KD*A and RbD*A and 90% or better for CsD*A. The Curie temperatures determined for these samples were 96.1 K (KDA), 110.1 K (RbDA), 143.0 K (CsDA), 159.8 K (KD*A), 169.8 K (RbD*A), and 202.8 K (CsD*A). These values are in general accord with previous values reported in the literature[21] with the exception of the value for CsD*A which is 9 K lower than the previously reported value. This value may reflect the lower limit on the level of deuteration for this salt.

III. RESULTS AND DISCUSSION

A. Molecular structure

1. Paraelectric phase

The primitive unit cells of both the paraelectric and ferroelectric phases of KDA and its arsenate isomorphs contain two formula units (16 atoms). In the paraelectric phase, the lattice belongs to the tetragonal crystal system and the structure transforms under symmetry operations according to the space group D_{2d}^{12} ($I\bar{4}2d$).[21] An analysis of the normal optic-vibration modes transforming as the various irreducible representations of the factor groups of these space groups at the Brillouin-zone center has been performed by Shur.[22] According to this, only those modes transforming as the A_2 representation are Raman inactive. Of the remaining representations, 4 A_1, 6 B_1, 6 B_2, and 12 E are Raman active, making a total of 28 Raman-active modes for the paraelectric phase.

Figures 1(a) to 1(e) present the measured Raman spectra in the range 10–3500 cm^{-1} for the four unique polarizations in the paraelectric phase of five of the six compounds. (We have omitted the spectra for KDA since these are basically similar to those reported previously by Agrawal and Perry.[17]) In each case the spectrum shown is that recorded at a few kelvins above the transition temperature, since such spectra generally present more detail and less ambiguity concerning the resonance frequencies (due to the breadth of the features) than are found in spectra recorded at higher temperatures. The frequencies of the features observed in these spectra (and for completeness for KDA) are summarized in Table I along with the irreducible representation of D_{2d} to which they have been assigned and the polarization in which that representation is observed.

The internal organization of Table I is based upon the morphological similarity of the various paraelectric spectra. Therein, all frequencies occupying the same horizontal line are deemed sufficiently alike in the different spectra to be assigned with confidence to the same origin. This, of course, does not preclude a similarity of origin for some of the other lines. For ease of reference, in the following text modes occupying the same horizontal line in Table I (and later in Table III for the ferroelectric phase) will be referred to as "counterparts" and designated by their symmetry.

A comparison between Table I and Figs. 1(a) to 1(e) should make the correspondence between tabulated frequency and spectral feature self-evident. There are, however, a few spectral pecularities which lead to ambiguity and should be discussed.

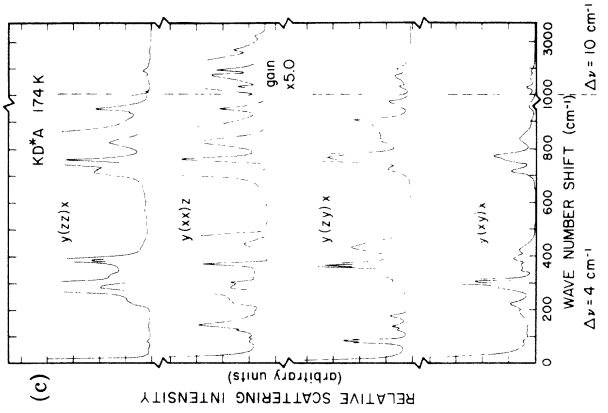

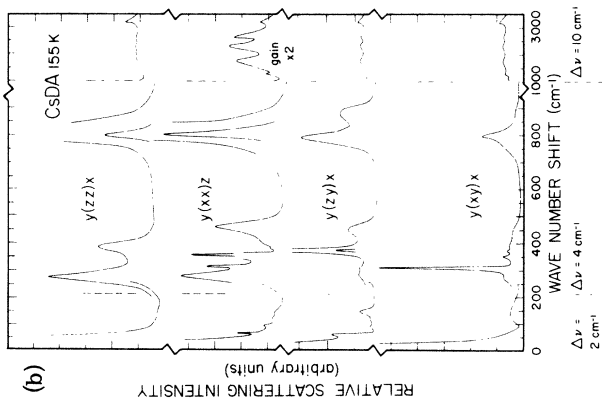

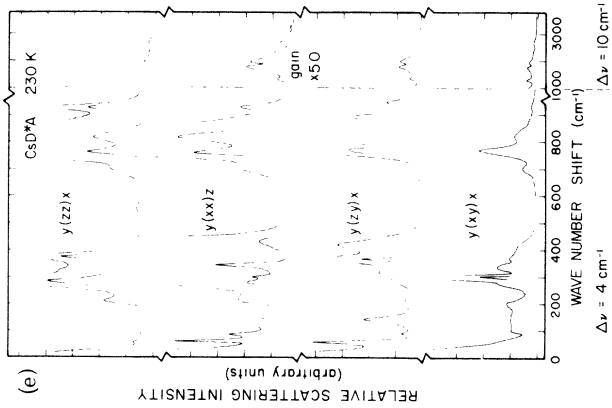

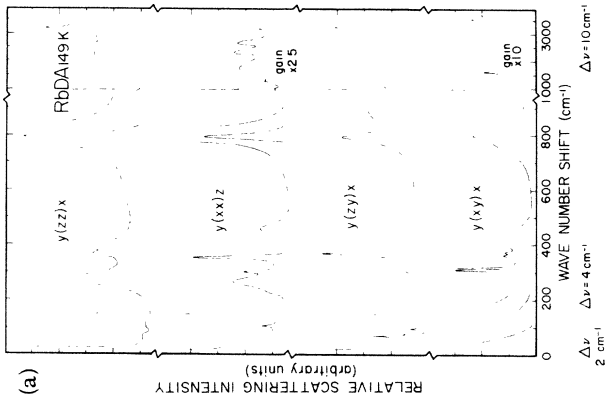

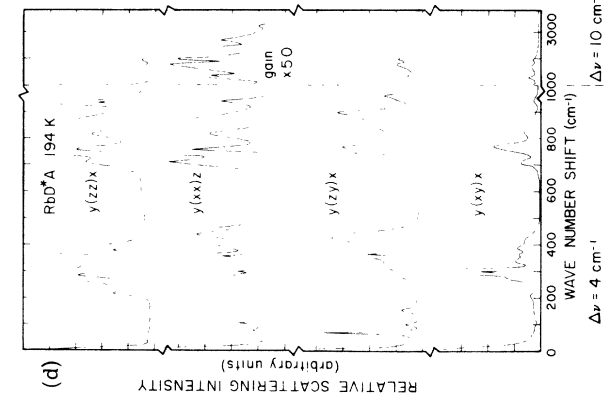

FIG. 1. Measured low-temperature Raman spectra in the range 10–3500 cm^{-1} for the four unique polarizations in the paraelectric phase of (a) RbDA, (b) CsDA, (c) KD*A, (d) RbD*A, and (e) CsD*A.

TABLE I. Frequencies (in cm^{-1}) of the observed features in the paraelectric spectra for the six arsenates measured just above the Curie temperature, along with the irreducible representation of D_{2d} to which they have been assigned and the polarization in which that representation is observed. All frequencies occupying the same horizontal line are considered to have the same origin (and are referred to as counterparts in the text). Note that the frequencies associated with the ferroelectric mode and the low-frequency B_2 phonon with which it interacts, which are determined from the coupled-harmonic-oscillator fits, are not included in this table.

KDA		124 K		RbDA		149 K		CsDA		155 K		KD*A		174 K		RbD*A		194 K		CsD*A		230 K	
A_1 (xx,zz)	B_1 (xx)	B_2 (xy)	E (xz)	A_1 (xx,zz)	B_1 (xx)	B_2 (xy)	E (xz)	A_1 (xx,zz)	B_1 (xx)	B_2 (xy)	E (xz)	A_1 (xx,zz)	B_1 (xx)	B_2 (xy)	E (xz)	A_1 (xx,zz)	B_1 (xx)	B_2 (xy)	E (xz)	A_1 (xx,zz)	B_1 (xx)	B_2 (xy)	E (xz)
			79				69				58	(45)			80	(33)			71				59
									63												59		
																	75						
													(90)										
			117				77								118				(81)				
			130				96				88				135				103				89
	135				135				137								105				87		
	143				106				91.5				138.5				140				125		
													158										
			175				159				143				171				156				140
														218				210				200	
												218				212				210			
															238				232				215
266				271				276				277				281				281			
														275				270				269	
															290				284				284
		308				308				308				298				296				300	
															318				317				313
														333				335				336	
	368				356				350				364				355				344		
			368				369				373				362				364				364
400				394				385				379				376				370			
														383				383				(383)	
		421				410				390				419				418				418	
			462				452				452				430				425				419
	470				462				454				439				435				430		
												555				550				549			
												712				709				696			
															721				711				693
												757				758				759			
															766				768				767
		746				760				755				770				768				768	
795				795				798				822				816				814			
														833				830				823	
			885				890				891				906				899				893
												946				938				924			
														955				940				930	
															972				961				943
	1320				1305				1268				1335				1330				1312		
	1800				1770				1782				1765				1740				1750		
													1955				1950				1930		
	2350				2330				2328				2385				2330				2313		
	2690				2675				2638				2668				2660				2650		

The first of these occurs in the A_1 symmetry of KD*A and RbD*A at 45 and 33 cm^{-1}, respectively. This feature is very weak and cannot be seen in the xx polarization for the remaining compounds and neither is it observable in any of the compounds at room temperature. As Fig. 2(a) shows, the KDA E spectrum in the vicinity of 100 cm^{-1} may be described as a sharp peak at 79 cm^{-1} with two more features at 117 and 130 cm^{-1} that appear very much like interference between two interacting phonons of the same symmetry; similar features are found for all the arsenates. It would be of interest to be able to fit this phenomenon to a coupled-oscillator system as is discussed later in the text for the B_2 spectrum at low frequencies. However, the interference region is clearly only a part of quite an extended interacting system of modes, including the 79- and 175-cm^{-1} bands. To fit these features to a system of four coupled damped harmonic oscillators is at present a nearly impossible task, especially since in RbDA and CsDA the system lies closer to the exciting line and some features apparently overlap; these latter comments are also true for the deuterated compounds. The feature at 135 cm^{-1} in KDA B_1 symmetry is very broad and weak but it appears in all three hydrogenated compounds and does not vary from compound to compound as do other modes of which it might be crosstalk; furthermore, this feature cannot be seen at room temperature. The 143-cm^{-1} feature in KDA B_1 symmetry and its counterparts in the other compounds are related in Table I because a similar feature always occurs in these spectra at about the frequency of the first minimum in the B_2 spectrum. The 218-cm^{-1} feature in KD*A B_2 symmetry and its counterparts in the deuterated materials appear as an additional peak at the high-frequency end of the interference spectrum. The 238-cm^{-1} feature in KD*A E symmetry and its counterparts are quite broad and weak but appear consistent and distinct in the deuterated data. The features found in KDA at 275 cm^{-1} in B_2 symmetry and 290 cm^{-1} in E symmetry and their associated counterparts appear as relatively small shoulders on the sides of much larger lines with consequently uncertain frequency locations, but their behavior from compound to compound indicates their probable reality; this 275-cm^{-1} band and its counterparts are not seen at room temperature. The 318-cm^{-1} feature in KD*A E symmetry and its counterparts are also observed as shoulders on the sides of stronger structures; this band is not observed in KD*A at room temperature. The 383-cm^{-1} feature in KD*A B_2 symmetry and its counterparts are part of a broad spectral feature but appear distinct at low temperatures; at room temperature it cannot be distinguished in KD*A. The 421-cm^{-1} feature in KDA B_2 symmetry and its counterparts are the final features of the broad region just described. They appear only in KDA and KD*A at room temperature. The 555-cm^{-1} feature in KD*A A_1 symmetry and its counterparts are extremely broad and weak although they remain visible even at room temperature. The 2385- and 2668-cm^{-1} features in KD*A B_1 symmetry and their counterparts in the deuterated compounds appear as very weak broad shoulders. The 800–900-cm^{-1} region in the E spectra of the deuterated samples contain a broad region of scatter but no really distinct features. This is not fluorescence but cannot be assigned a specific frequency. Finally, a recurring feature at 3200 cm^{-1} is an instrumental artifact.

The interpretation of these spectra may be roughly divided into four parts, on the basis of whether a given mode is associated with a protonic or deuteronic motion, a lattice vibration, an internal mode (of an AsO_4^{3-}, $H_2AsO_4^-$, or $D_2AsO_4^-$ ion) or a vibration of the hydrogen or deuterium bonds. In general, these may be expected to occur in order of increasing frequency.

A distinctive feature of collective protonic motion[2,3] as opposed to the Slater-type random thermal excitation across a potential barrier,[23] apart from the isotope effect, is the existence of these motions as distinct lattice-type vibrations observable in this case as low-frequency Raman-scattered lines. There are four such modes which exist as a B_2, a doubly degenerate E, and an A_2 vibration.[24] The Slater model leads to a Debye susceptibility for the proton motion while Kaminow and Damen demonstrated that the scattering in the low-frequency region under B_2 symmetry is better described as an overdamped harmonic oscillator with constant friction damping.[25] Subsequent investigations have removed the ambiguity in the temperature dependence determined for this phonon by treating the scattering as a result of two interacting B_2 modes, one a transverse optic phonon and the other the soft overdamped ferroelectric mode.[26] This treatment has been extended to other materials[19,20,27] and is used here in a later section to describe the low-frequency B_2 spectra obtained in the present work. Lavrenčič *et al.*[28] first proposed the existence of the mode of E symmetry as a broad feature at the low-frequency end of the scattered spectrum for that symmetry in KDP and KD*P. This feature has been treated by Scott and Wilson[29] as an E-symmetry projection of the one-phonon density of states in the low-frequency region for $\tilde{q} \approx 0$ for KDP with the usual wave-vector conservation relaxed by protonic disorder. Broberg *et al.*[30] treated a similar feature in $NH_4H_2PO_4$ as the E-mode polarization fluctuation mentioned above. Either treatment is complicated here by the multiplicity of modes in this region [see Figs. 2(a) and 2(b)] which appear to interact with the broad feature

as mentioned earlier. A simplified attempt has been made for KDA, the easiest case, to fit this feature with just two interacting oscillators. The results of this attempt suggest an overdamped E mode located at approximately 150 cm^{-1} at room temperature. However, the complicated nature of the spectra prohibit a more precise determination of the frequency and its temperature dependence. The remaining protonic mode, of A_2 symmetry, would of course be unobservable in a Raman-scattering experiment.

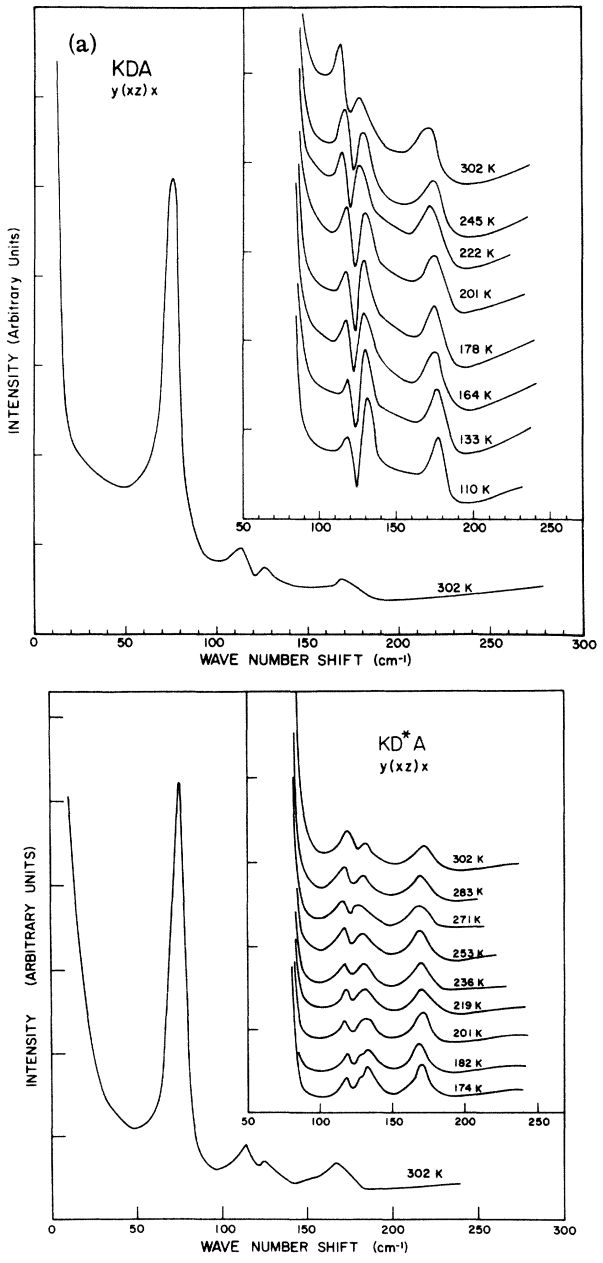

FIG. 2. Measured temperature dependence of the low-frequency E spectra for (a) KDA and (b) KD*A in the paraelectric phase showing the apparent interference between interacting phonons in this symmetry.

Shur[31] has, on the basis of a group-theoretical analysis founded on the assumed space groups D_{2d}^{12} and C_{2v}^{19}, enumerated the type of mode and the number of times it may be expected to occur as a given basis for D_{2d} or C_{2v} in these isomorphs. This is reproduced in Table II. He has also calculated the expected frequency values for KDP of the transverse-optic lattice modes,[32] that is, the vibrations of the K^+ ion against the $H_2PO_4^-$ ion, at $\vec{q} \approx 0$. The frequencies of these modes (and their symmetries) are ~5 cm^{-1} (B_1), 68 cm^{-1} (E), 99 cm^{-1} (E), 118 cm^{-1} (E), 135 cm^{-1} (B_1), and 187 cm^{-1} (B_2). These compare reasonably well with experimental results[17,18,33,34] subject to a qualification on the interpretation of the low-frequency B_2 spectra. The proper frequency for the low-frequency B_2 mode should be derived on the basis of a fit to the data involving the interacting modes, as discussed in a later section of this work. Substitution of As for P will change the reduced mass of the KDP system by less than 9% and will presumably have even less effect on the intermolecular forces. Therefore, the frequencies calculated for KDP should be reasonable values with which to compare those found for KDA. No very low-frequency B_1 mode is observed, but one below 10 cm^{-1} would not have been using our experimental equipment and neither has the analogous mode been observed by the work referenced above on KDP.[17,18,32,33] Another calculation has been made by Fujiwara[9] which further substantiates the likely existence of a very low-frequency B_1 mode. The three lowest-frequency E modes in KDA have frequencies of 76, 113, and 125 cm^{-1} at room temperature which do not present an unreasonable comparison with the calculated values. Although higher in frequency than the calculated values, they are lower than the analogous experimental values determined for KDP.[17,18,33,34] The lowest B_1-mode frequency observed at low temperatures in KDA in the paraelectric phase is at 135 cm^{-1}. This mode, however, is not observed to depend on cation mass as could be expected and it also fails to appear in a recognizably similar form in the deuterated compounds and cannot be observed at room temperature. Therefore, we believe that the next-highest B_1 mode may be assigned to the B_1 symmetry translational optic lattice mode discussed by Shur; at room temperature in KDA this mode is at 135 cm^{-1} which is to be compared against a calculated value of 135 cm^{-1} for KDP. Finally, accepting the frequency of the underdamped mode obtained from a coupled oscillator fit as that of the remaining lattice mode of B_2 symmetry (see the later discussion on this subject), we find a frequency of 146 cm^{-1} at room temperature in KDA which is to be compared to the calculated value of 187 cm^{-1} for KDP.

In analogy with the calculations given for KDP in Table II, there should be three observable librational modes ($2E + A_1$) of the $H_2AsO_4^-$ or $D_2AsO_4^-$ complexes. These would be expected to be of lower frequency than the internal modes of vibration of the AsO_4^{3-} ion. In the absence of calculated values, however, any frequency assignments must be speculative. The 266-cm^{-1} band found in KDA A_1 symmetry and its counterparts have a strong anomalous temperature dependence (being, at room temperature, at 287, 285, 285, 285, 284, and 282 cm^{-1}, respectively, for the six compounds in order of increasing atomic weight, which are to be compared against the low-temperature values given in Table I). In view of the room-temperature values for this feature, it is also apparently independent of the cation mass. If this mode were to be assigned the role of libration, this latter phenomenon would be explicable since the A_1 libration involves no motion of the cation but does involve a considerable stretching of the O–H–O or O–D–O bonds.[22] This assignment must remain doubtful, however, since there is a considerable dependence on the substitution of As for P (at room temperature the mode moves from 287 cm^{-1} in KDA to 360 cm^{-1} in KDP[17]) and these atoms should not be significantly involved in the libration.[22]

Under the T_d symmetry of the free AsO_4^{3-} ion, its normal vibrations transform according to the bases E (doubly degenerate), F_2 (triply degenerate), A_1 (singly degenerate), and F_2 (triply degenerate) in order of increasing frequency. An alternate origin for the 266 cm^{-1} feature found in KDA A_1 symmetry and its counterparts discussed in the previous paragraph could be the ionic motion of E symmetry. This would account for the mass dependence displayed by this feature. According to an earlier analysis performed on KDP spectra,[34] this 266-cm^{-1} feature and one of B_2 symmetry at 308 cm^{-1} in KDA would correspond to a splitting of the lowest AsO_4^{3-} mode under the S_4 site symmetry of the ion. Again, however, as for the previous interpretation, the anomalous temperature dependence of the 266-cm^{-1} line is not readily explicable in these terms, especially since the 308-cm^{-1} line has very little temperature dependence (being, at room temperature, at 306, 298, 306, 296, 306, and 299 cm^{-1}, respectively, for the six compounds in order of increasing atomic weight). Nevertheless, the assignment suggested here for the E mode of the AsO_4^{3-} ion compares well with frequencies deduced for the arsenate ion free, in solution, and in KDA.[35] To continue this manner of assignment, a careful comparison of the spectra of KDA and KDP[17,18] indicates that the modes assigned to the F_2 ion vibration would be the 368 cm^{-1} (E_1) and 368 cm^{-1} (E) vibrations in KDA. The A_1 ionic vibration would then be the 795-cm^{-1} A_1 vibration in KDA while the highest-frequency F_2 ionic mode appears in E symmetry at 885 cm^{-1} in KDA. According to the above, one would expect to see the third mode of the split F_2 mode in B_1 symmetry, but none is observed. However, the original F_2 mode when split by the S_4 site symmetry may also become a B_2 mode in the D_{2d} lattice. Indeed, a B_2 mode is observed at 746 cm^{-1}. Thus this band and the 885-cm^{-1} line found in E symmetry in KDA could be the 810-cm^{-1} free-arsenate vibration[35] split by the crystal field. Thus while at lower frequencies the spectra are consistent with an almost free AsO_4^{3-} ion at an S_4 site, the higher-frequency splitting implies a greater degree of correlation between ionic motion.

The diffuse bands above 1000 cm^{-1} in the paraelectric phase, which have been assigned B_1 symmetry, are in the frequency region expected to be occupied by O–H–O or O–D–O deformations[36] and have been ascribed to this origin by several workers on KDP,[17,37] KD*P and KDA,[17] RbDP[38,39] and RbDA.[38] A careful comparison of the relative intensities of these high-frequency features found

TABLE II. The numbers of lattice, libration, and internal modes of KDA and its isomorphs, and the irreducible representations according to which they transform (Ref. 31). T represents temperature, T_c is the transition temperature, and the internal modes are those of the $H_2AsO_4^-$ or $D_2AsO_4^-$ ion.

Symmetry	Representation	All modes	Lattice (acoustic)	Lattice (optic)	Libration	Internal
	A_1	4	0	0	1	3
($T > T_c$)	A_2	5	0	0	1	4
D_{2d}^{12}	B_1	6	0	2	0	4
	B_2	7	1	1	0	5
	E	13	1	3	2	7
	A_1	11	1	1	1	8
($T < T_c$)	A_2	11	0	2	1	8
C_{2v}^{19}	B_1	13	1	3	2	7
	B_2	13	1	3	2	7

for the arsenates proves to be consistent with this earlier work and reveals the three principal features in KDA to be at 1800, 2350, and 2690 cm^{-1}. The ratio of a line frequency in the hydrogenated sample to its counterpart frequency in the corresponding deuterated sample yields the values of 1.35, 1.33, and 1.38, respectively, in order of increasing frequency for these three principal lines, which is close to the square root of the deuterium to hydrogen mass ratio. Furthermore, the variation of the equivalent ratios for the Rb and Cs compounds and of any dependence on temperature is less than 1.5% of the above values. Such results strongly suggest that the O–H–O or O–D–O deformations are associated with these three principal bands above 1000 cm^{-1}. Finally, it is pointed out that the two highest frequencies tabulated for the deuterated materials are much reduced in intensity, existing as barely discernible shoulders. It is possible that these modes are the remnants of the two highest-frequency modes found in the hydrogenated samples and are a result of incomplete deuteration.[37]

In reviewing the discussion so far we note here that, first, several spectral lines are unaccounted for, second, that more B_1 modes are observed than are group theoretically predicted, and finally that the librational modes have not been positively identified. With respect to the latter, it does not seem possible to accomplish this since several E modes and one A_1 are not seen (in the hydrogenated samples at least) so that the librational modes could remain entirely unobserved.

The remaining features must still be accounted for in terms of their possible reality as first-order Raman scatter. The 135-cm^{-1} feature found in KDA B_1 symmetry and its counterparts are not observed at room temperature and not at all in the deuterated compounds and it seems likely that they may not be first-order Raman lines. The feature at 175 cm^{-1} in KDA E symmetry and its counterparts are clearly distinct modes, possibly one of the libration frequencies. Of the remaining unidentified modes, only the existence of the 421-cm^{-1} feature in KDA B_2 symmetry and its counterparts can be seriously questioned. It generally comprises a broad spectral region of ill-defined detail, in the same frequency range where several features coexist in other polarizations. This feature, then, could be crosstalk from these polarizations accompanied by some second-order scatter. This feature is not observed at room temperature in RbDA and CsDA. We are left, then, with an excess over group-theoretical predictions of at least one in the number of B_2 modes. Previous workers[37] have observed a feature at 1295 cm^{-1} in KDP which may be the counterpart of the 1320-cm^{-1} B_1 feature in KDA (and its counterparts in the arsenates); spectra recorded for partially deuterated KDP reveal a weakening in intensity of this mode and the appearance of a mode at 985 cm^{-1} in A_1 symmetry which we believe may be the counterpart of the 946-cm^{-1} feature found in KD*A A_1 symmetry. Interpretation was not attempted in the earlier work, but it seems likely from the present work that these features in the deuterated and hydrogenated compounds correspond to deuteronic or protonic motions. In the work on KDP the ratio of the frequency for this feature in the hydrogenated sample to that in the deuterated sample was ~1.32, which is close to the square root of the deuterium to hydrogen mass ratio. In the present case, the appropriate ratios are 1.39, 1.39, and 1.37 for the K, Rb, and Cs salts, respectively, which compare favorably with the ratios determined for the higher-frequency protonic and deuteronic motions discussed earlier. One significant consequence of these observations is that the 946-cm^{-1} line found in KD*A and its counterparts in the deuterated samples are definitely of A_1 symmetry. This could imply that their counterparts in the hydrogenated compounds are also of A_1 symmetry with a zz component of the Raman tensor too small to be observed, especially in view of the weakness of the line in the xx spectrum. If this symmetry assignment is taken to be the case, then the number of observed B_1 modes in the hydrogenated samples will have been reduced to the proper number, six, as well as the number of observed A_1 modes increased to the proper number, four.

Shur[22] has shown that the valence vibrations of the protons would transform as B_2 symmetries, providing that there was a correlation between the motions of all four protons in the unit cell. That no B_2 or E modes are observed in the high-frequency region is indicative that no such full correlation is present. A complete lack of correlation in the proton motions would result in a spectrum of vibrations possessing $A_1 + B_1$ symmetry. These B_1 motions have been observed as outlined above, thus confirming the lack of coordination, but no A_1 contributions were seen. Earlier[38] work has indicated the presence of the A_1 modes at very slightly shifted frequencies, possessing no zz component of the Raman tensor. We have not attempted to observe these modes in the present work; such an observation would require crystals, cut with faces perpendicular to the [110] direction.[38]

A large number of additional features are seen in the paraelectric deuterated spectra relative to the hydrogenated spectra. Shur[22,31] has pointed out that if the correlation between protonic motion has little effect in splitting the ionic normal vibration frequencies, the number of distinct observable modes in the paraelectric phase will be reduced from 28 to 23. Thus, one might propose that an

increase in the effects of such a correlation for the deuterated samples would result in the proliferation of lines. One must approach these data with caution, however, since, first, many of the new lines are quite weak, rather than being an obvious split of a distinct feature, and second, the deuteronic motion is still observed in B_1 symmetry—consistent with uncorrelated motion. In fact, the only feature which truly appears to be split by deuteration is that at 795 cm^{-1} in KDA A_1 symmetry which becomes 757 and 822 cm^{-1} in KD*A A_1 symmetry; equivalent splittings for the counterparts of the 795-cm^{-1} KDA line in the other arsenates are also found. Of the remaining bands in the deuterated samples which seem uncorrelated with features of the hydrogenated spectra, the weaker have been described at the beginning of this discussion. In addition, the 218- and 712-cm^{-1} features in KD*A A_1 symmetry and the 721-cm^{-1} feature in KD*A E symmetry and their associated counterparts appear as distinct satellites to higher frequency, much more intense lines. Further, the 45-cm^{-1} line in KD*A A_1 symmetry and its counterparts are not seen in the xx polarization and are not present at all at room temperature. Finally, the 333-cm^{-1} line in KD*A B_2 symmetry and its counterparts are parts of a complex of weak lines which cannot be accounted for by crosstalk. Precise interpretation of this multitude of lines is impossible but it is conceivable that many of the weaker lines are nonzero center scattering allowed by momentum-conservation breakdown mediated by deuteron disorder as proposed by Scott and Wilson[29] to account for the low-frequency E-mode spectrum of KDP.

2. *Ferroelectric phase*

Upon transition to the ferroelectric phase, the crystal system of the ferroelectric arsenates becomes orthorhombic and the space group C_{2v}^{19} ($Fdd2$).[21] In the ferroelectric transition, A_1 and B_2 modes of the paraelectric phase become A_1 modes under C_{2v} symmetry, A_2 and B_1 become A_2, and E modes split into B_1 and B_2 modes.[31] In the ferroelectric phase, all modes ($10A_1$, $11A_2$, $12B_1$, and $12B_2$) are Raman active, making a total of 45.

Figures 3(a) to 3(f) show the measured Raman spectra recorded in the ferroelectric phase for the six compounds. It should be noted that one supposedly unique polarization has been omitted from Fig. 3. In all cases, the zy polarization has been examined as well as xz, but in no case has a significant difference, other than over-all intensity, been observed between them. This is due to the domain structure observed in these materials in the ferroelectric phase and to the orientation of the new x', y' axes which align themselves approximately along the original [110] axes. Thus, in a right-angled scattering geometry, $y(zz)x$ (using tetragonal axis directions) will give a purely zz spectrum; $y(zy)y$ will give zy' and zx'; $y(xy)x$ will give $ax'x' - by'y' + cx'y' - dx'y'$, where the coefficients a to d depend on domain size, orientation, and crystal properties. Thus, in general, the $y(xy)x$ spectrum will contain information on A_1 and A_2 modes. Even if this situation were altered by changing the scattering geometry, however, the size of the domains renders it very difficult, if not impossible, to get a "clear" spectrum because of birefringence and internal reflections. In practice, the A_1 and A_2 modes are always separable between themselves and from B_1 and B_2 modes, and the problem is little greater than that of ordinary crosstalk discussed earlier for the paraelectric spectra.

The frequency values of the spectral features shown in Figs. 3 are summarized in Table III along with the irreducible representation of C_{2v} to which they have been assigned and the polarization in which that representation is observed. The organization of Table III follows that described earlier for the preparation of Table I. Apart from some very weak lines of questionable existence, which have been indicated by means of parentheses in Table III, only a few comments need be made about the tabulation of data. The 366-cm^{-1} (A_1) and 372-cm^{-1} (B_1, B_2) features observed in KDA can be resolved in RbDA but not in CsDA. The ordering of frequencies 431–453 cm^{-1} in CsDA A_1 and B symmetries has been made on the relative intensity of the components. Features at 730 cm^{-1} in KDA A_1 symmetry and at 865 cm^{-1} in KDA B_1, B_2 symmetry may be spurious as both are very weak broad shoulders on much larger bands and do not appear in the spectra of the isomorphs.

We have been able to identify most of the lattice and internal modes contributing to the ferroelectric spectra. The lowest-frequency ferroelectric B_1 mode, which will now transform according to A_2 symmetry, is still not observable and broadening of the central lines of the spectra for A_2 symmetry, which would indicate its existence at very low frequency, is not observed. The B spectra in the ferroelectric phase display several low-frequency features which correlate well with the frequencies observed for the low-frequency transverse optic modes of E symmetry in the paraelectric phase. The number of such modes does not increase for KDA, indicating minimal splitting between the B_1, B_2 modes. In the other compounds, the 78-cm^{-1} feature in RbDA E symmetry and its counterparts is the only additional frequency to be observed, suggesting that only the lowest-frequency transverse optic mode of E symmetry is split. The 193-cm^{-1} ferroelectric feature in KDA A_2 symmetry and its counterparts correspond to the lowest transverse optic mode of B_1 symmetry observed

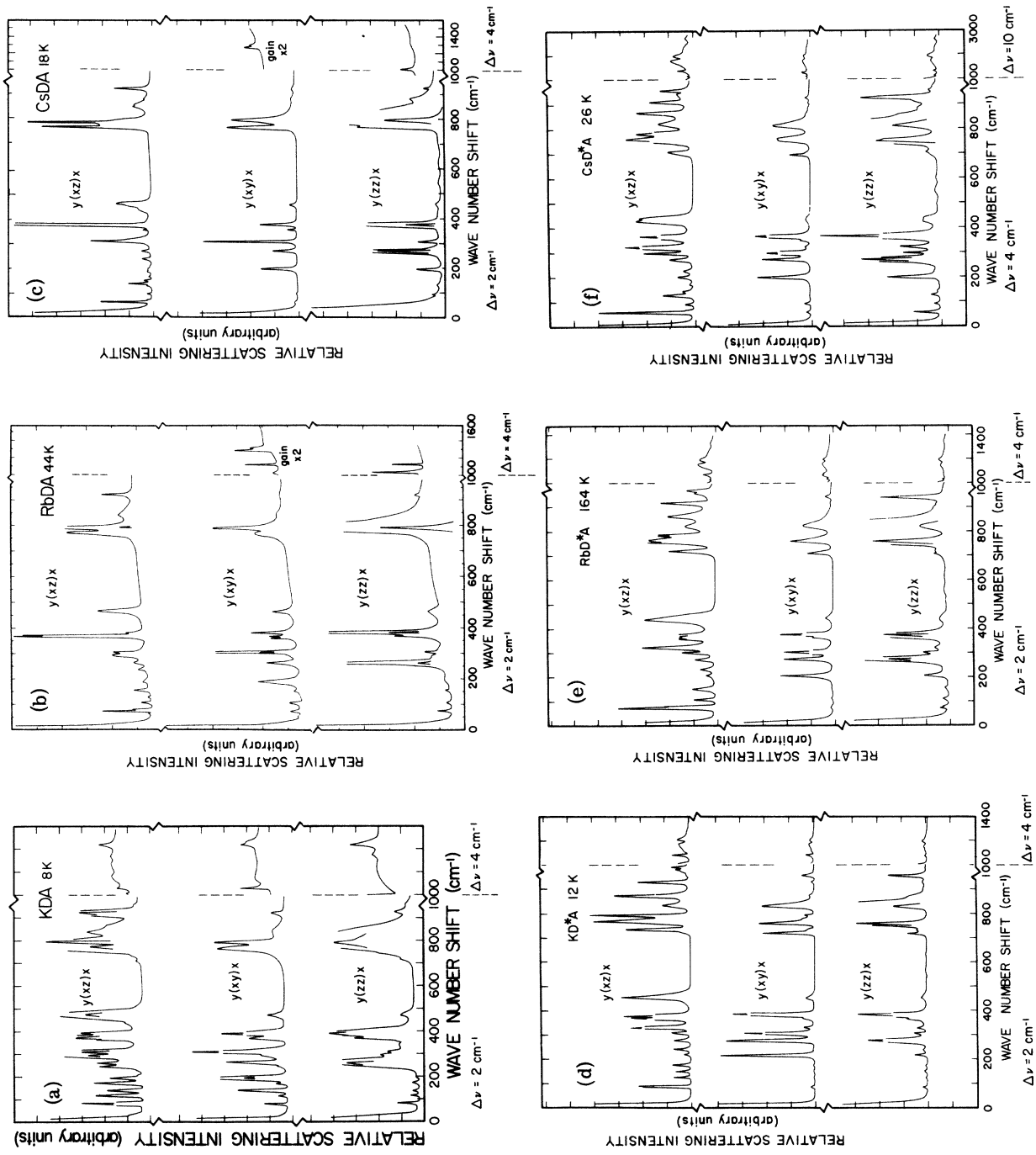

FIG. 3. Measured Raman spectra in the range 10–3500 cm^{-1} for the ferroelectric phase of (a)KDA, (b) RbDA, (c) CsDA, (d) KD*A, (e) RbD*A, and (f) CsD*A. The spectra for the (zy) polarization are not included since in no case do we observe any significant difference, other than over-all intensity, between these spectra and those recorded in (xz).

TABLE III. Frequencies (in cm^{-1}) of the observed features in the ferroelectric spectra measured for the six arsenates, along with the irreducible representation of C_{2v} to which they have been assigned and the polarization in which that representation is observed. All frequencies occupying the same horizontal line are deemed to have the same origin.

KDA		74 K	RbDA		44 K	CsDA		18 K	KD*A		12 K	RbD*A		20 K	CsD*A		26 K
A_1 (zz)	A_2 (xy)	B_1, B_2 (xz)	A_1 (zz)	A_2 (xy)	B_1, B_2 (xz)	A_1 (zz)	A_2 (xy)	B_1, B_2 (xz)	A_1 (zz)	A_2 (xy)	B_1, B_2 (xz)	A_1 (zz)	A_2 (xy)	B_1, B_2 (xz)	A_1 (zz)	A_2 (xy)	B_1, B_2 (xz)
		80			73			62			78			73			57
					78			70			80			79			(65)
		115			106			95			118			108			90
															94		
		136			128			126			139			132			127
	(138)																
									(147)			(141)					
		169			155			135			167			150			142
								(148)									173
								(174)									
	193			189			195			210			205			201	
		240			236			236			232			232			226
258			262			267			269			270			271		
		293			293												
	307			304			306			299			297			298	
											322			321			321
											358			360			362
											367			367			365
(340)																	
				359			352										
		366			361												
		372			372												
								368									
388			382			373			375			372			364		
		455			447			431									
		468			467			461									
		481			477			453									
											444			438			429
																	438
						(545)											
						(619)											
										711			708			697	
											728			728			727
(730)																	
									754			756			753		
											762			759			760
	761			765			767										
		771			771			770									
											785			782			779
788			791			795											
									824			816			815		
		796			795			789									
		837			841			851									
								858									
		(865)															
						883											
											863			861			859
											920			912			909
		923			922			925									
1050			1025			1011											
									947			940			925		
											969			958			941
											980			970			956
																	1115
																	1255
	1305			1280			1269			1290						1275	
	1335			1315			1297			1315			1280				
		1785			1825			1765			1355			1350			1325
											1795			1785			1735
											1940			1935			1920
		2325			2370			2270									2290
		2665			2655			2630									2625

in the paraelectric phase. The 169- and 240-cm^{-1} ferroelectric features in KDA B symmetry and their associated counterparts most likely correspond to the 175-cm^{-1} paraelectric feature in KDA E symmetry and its counterparts. The 258-cm^{-1} ferroelectric feature in KDA A_1 symmetry and its counterparts correspond to the 266-cm^{-1} paraelectric feature in KDA A_1 symmetry and its counterparts. The 307-cm^{-1} ferroelectric feature in KDA A_2 symmetry and its counterparts should correspond to the 308-cm^{-1} paraelectric feature in KDA B_2 symmetry and its counterparts but appears under the wrong symmetry to do so. The identification seems to be well supported by the data, however, and agrees with previous work[17] so there is some apparent ambiguity. It is possible that the degree of correlation of the ionic motion changes, resulting in a collective mode of different symmetry than expected. The 368-cm^{-1} paraelectric features in KDA B_1 and E symmetry and their associated counterparts, identified with the lowest triply degenerate F_2 ionic mode, have no clearly consistent analogs in the ferroelectric phase. The ferroelectric spectra of all samples display features in E symmetry over the frequency range 350–375 cm^{-1} which cannot be clearly related on the basis of spectral similarity. They are of suitable frequency to be the analogues of the 368-cm^{-1} paraelectric features in KDA E symmetry and its counterparts, however, and this would indicate that these features are split in the ferroelectric phase. An A_2 mode corresponding to the 368-cm^{-1} paraelectric feature in KDA B_1 symmetry and its counterparts is not observed in the ferroelectric phase of KDA or the deuterated materials, but the 359-cm^{-1} feature in ferroelectric RbDA A_2 symmetry and its counterpart in CsDA do correspond to the B_1 feature observed in their paraelectric phases. The modes identified with the A_1 symmetric ionic internal motion in the paraelectric phase are again observed at 788 cm^{-1} in the KDA A_1 ferroelectric symmetry and its counterparts in the hydrogenated samples, and at 754 and 824 cm^{-1} in KD*A A_1 ferroelectric symmetry and its counterparts in the deuterated samples. The highest B_2 and E modes for the compounds in their paraelectric phase, which were assigned to the highest triply degenerate F_2 mode of the AsO_3^{3-} ion, have counterparts under B symmetry in the ferroelectric phase, although the multiplicity of lines makes it difficult to differentiate between the split ionic mode and other modes, possibly observed in the ferroelectric but not in the paraelectric phase. Once again, the 746-cm^{-1} paraelectric feature in KDA B_2 symmetry and its counterparts appear in the ferroelectric phase, not as an A_1 mode but as an A_2 mode at 761 cm^{-1} in KDA and its counterparts.

The large linewidths noted above the transition disappear, strongly suggesting that they are indeed related to proton (deuteron) disorder, either through proton-phonon coupling or a relaxation of conservation of momentum due to the disorder. Other workers[39] have observed an increase in intensity of the high-frequency features ascribed to protonic motion when the ferroelectric transition is made. Although the intensities observed here did increase, on the average, by a factor of 2 between room temperature and the transition, the intensities below the transition were considerably lower, although the frequencies of the bands can be seen to vary little. The most interesting point is their appearance in B_1, B_2 symmetry. This is in apparent contradiction with previous work but seems strongly indicated. This would be consistent with the symmetry expected if the proton (deuteron) motions were correlated. The appearance of this spectral region in the undeuterated samples is very similar to that of the paraelectric phase, and is not shown in the appropriate figures in order that the wave-number region just above 1000 cm^{-1} may be presented in greater detail. The feature at 1320 cm^{-1} in KDA-xx which was attributed to a protonic motion now appears to be split. No splitting is observed, however, in the corresponding modes in the deuterated samples.

B. Ferroelectric mode

In the hydrogen-bonded ferroelectrics of the KDP family there are four tunneling protons in the primitive unit cell of the paraelectric phase whose vibrations belong to a B_2, a doubly degenerate E, and an A_2 species. Of these vibrations the B_2 and E proton modes are Raman active and would be expected to couple to optical phonons of the same species according to the Kobayashi theory.[4] Kaminow and Damen[25] first observed the ferroelectric soft mode in KDP by fitting the low-frequency Raman scattering in B_2 symmetry to a damped harmonic-oscillator form. Later investigations[26] have removed the ambiguity in the temperature dependence educed for this phonon by treating the scattering as a result of two interacting B_2 modes, one a transverse-optic phonon and the other the ferroelectric soft mode.[19] Similar investigations on hydrogen-bonded ferroelectrics have revealed the ferroelectric soft mode in B_2 symmetry in KDA and CsDA,[19] KD*P,[10] RbDP,[27] and, in a preliminary report of the present work, in RbDA.[20] We now present our findings for the whole arsenate family.

For all of the ferroelectric arsenates investigated here we observe a distinct broadening or shoulder close to the exciting line in the xy spectra which is not observed in other orientations. Figure 4(a) to 4(f) demonstrates this for the six arsenates. As the figure shows, this broadening or shoulder is markedly temperature dependent mov-

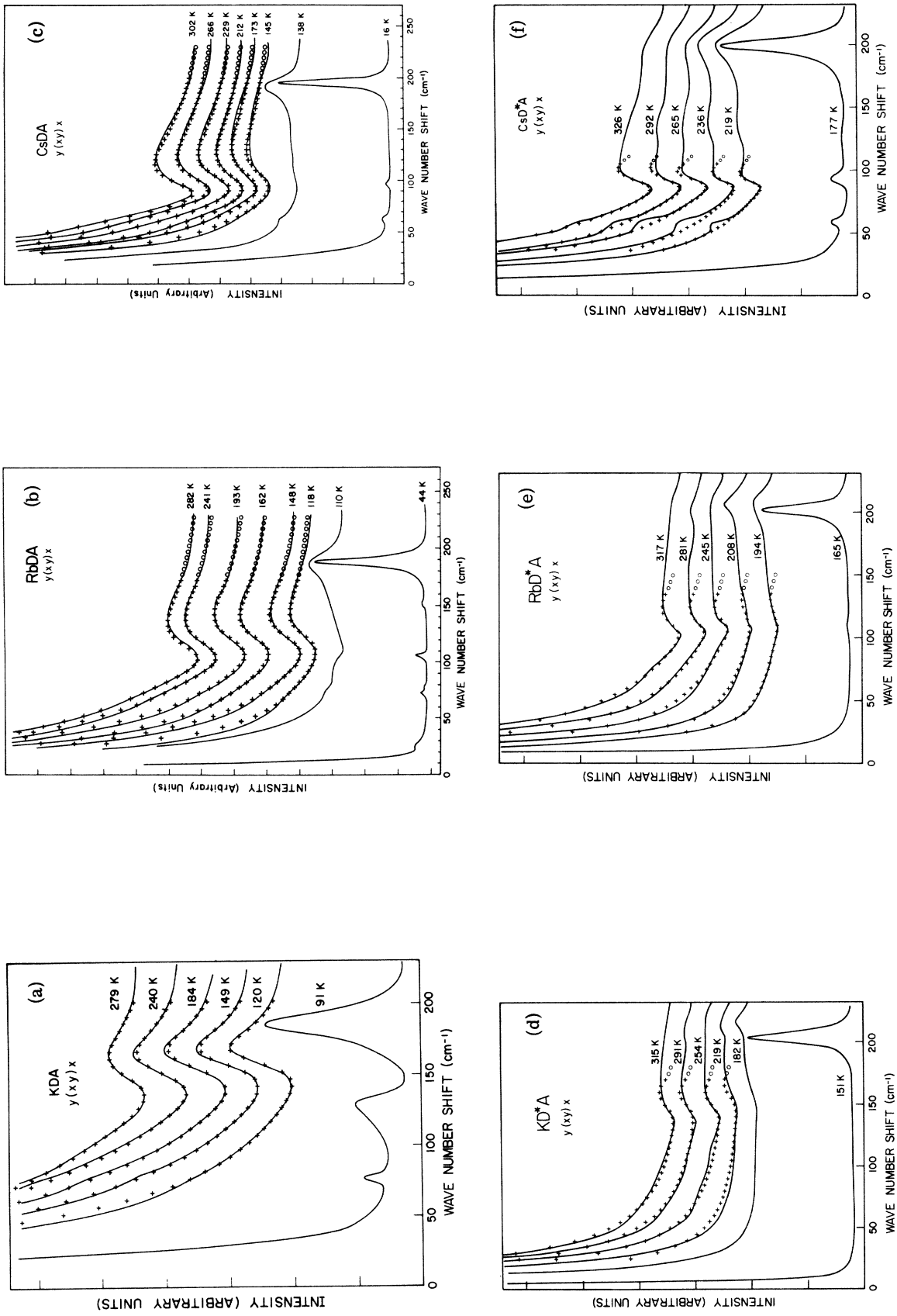

FIG. 4. Measured temperature dependence of the low-frequency B_2 spectra for (a) KDA, (b) RbDA, (c) CsDA, (d) KD*A, (e) RbD*A, and (f) CsD*A. The data points + are from the real coupled oscillator final fits. The data points O are extensions of the coupled oscillator fits beyond the input spectral frequency range.

ing closer to the exciting line with decreasing temperature. Furthermore, in the deuterated samples this feature is significantly closer to the exciting line than in the analogous hydrogenated sample. For these reasons we believe this feature is associated with the ferroelectric mode in these materials. In addition, these spectra reveal an antiresonant interference between the ferroelectric mode and a low-frequency B_2 phonon for the hydrogenated compounds. For the deuterated compounds the interference appears to involve two or more low-frequency phonons.

Following Katiyar *et al.*[19] we have attempted to fit these low-frequency xy spectra in terms of two coupled damped harmonic oscillators in order to determine the ferroelectric-mode frequency and its temperature dependence. The scattered power at a frequency shift ω due to a fluctuation in the α_{xy} component of the polarizability tensor induced by a lattice polarization fluctuation δP_i is given by

$$J(\omega) = C[n(\omega)+1]\chi''(\omega), \tag{1}$$

where C is an experimental constant, the n are the phonon population factors, and $\chi''(\omega)$ is the imaginary part of the complex susceptibility. For the coupled system,

$$\chi''(\omega) = \mathrm{Im}\sum_{ij} P_i P_j G_{ij}(\omega), \tag{2}$$

where P_i is the strength of the mode i and $G_{ij}(\omega)$ are solutions to the coupled equations given in Eq. (3)

$$\begin{pmatrix} \omega_i^2 - \omega^2 - i\omega\Gamma_i & \Delta^2 - i\omega\Gamma_{ij} \\ \Delta^2 - i\omega\Gamma_{ij} & \omega_j^2 - \omega^2 - i\omega\Gamma_j \end{pmatrix} \begin{pmatrix} G_{ii} & G_{ij} \\ G_{ij} & G_{jj} \end{pmatrix} = \begin{pmatrix} 1 & 0 \\ 0 & 1 \end{pmatrix} . \tag{3}$$

Equations (3) are overdetermined allowing an arbitrary choice of diagonalization. The two limiting cases occur for real coupling, that is with $\Gamma_{ij} = 0$, or for imaginary coupling with $\Delta^2 = 0$. There are, of course, an arbitrary number of equivalent intermediate forms involving both kinds of coupling which are obtained by using the appropriate unitary transformations that diagonalize neither the real nor imaginary coupling matrices. In the present work we have used only the two limiting cases of real or imaginary coupling and have determined the remaining parameters in Eq. (3) by a computer least-squares fit to the low-frequency xy spectra. The curve-fitting technique utilized either the usual Taylor-expansion method to second order or the method of steepest descent to minimize the sums of the squares of the differences between the observed and calculated data. The data values were weighted by their inverse squares in order to adjust for the most likely inaccuracies in the data and to ensure that the variance was independent of scale. For the hydrogenated compounds the fits were made to the spectra in the 10–230-cm^{-1} range. For the deuterated compounds, however, the presence of a third oscillator can be seen around 200 cm^{-1} and for CsD*A there may be a further oscillator near 140 cm^{-1} (together with a feature at 55 cm^{-1}). Because of the 16 parameters involved, we have not been successful in meaningfully describing the deuterated system by a three-coupled oscillator system. In addition, results were not satisfactory from a two-coupled oscillator system with a third uncoupled oscillator. We have, therefore, attempted to ignore the influence of the third (and any other) oscillator by fitting the data for the deuterated compounds only in the spectral range 10–130 cm^{-1} with the two-coupled-oscillator system. However, we were unable to achieve acceptable fits to the KD*A low-temperature data even in this restricted range. In general, the weighted variance of all the fits achieved were of the order of 10^{-3}–10^{-4}, while the standard error for the individual parameters characterizing the two oscillators was of the order of a few percent. The quality of the fits can be assessed from Fig. 4(a) to 4(f) in which data points arising from the final fits are shown superimposed on the low-frequency xy spectra.

Tables IV and V itemize the educed values of ω_i and Γ_i for the two coupled modes determined for the separate cases of real and imaginary fits to the xy spectra for the six arsenates; note that we use the subscripts a and b to distinguish between the two oscillators in the presence of real coupling, and α and β when imaginary coupling is utilized. For the presence of real coupling, Table IV shows that, for each arsenate, mode a is a soft overdamped mode, while mode b exhibits the conventional temperature dependence of a normal phonon. In all cases it can be seen that there is a systematic trend to lower frequencies of mode b as the cation mass is increased in either the hydrogenated or deuterated series. Furthermore, the process of deuteration leads to a significant decrease in the mode-a frequency for a particular cation, but has relatively little effect on mode b. It is to be noted that the values of Δ^2 are not small in comparison to either ω_a or ω_b but are not very temperature dependent; the process of deuteration generally leads to a lowering of Δ^2. For real coupling fits, we therefore interpret mode a as the ferroelectric mode and mode b as a low-frequency B_2 phonon.

The parameters characterizing the two modes in the presence of imaginary coupling are simply determined via the appropriate unitary transformation[40] from the corresponding parameters educed

TABLE IV. Values (in cm^{-1}) of ω_a, ω_b, Γ_a, Γ_b, and Δ determined from the coupled-harmonic-oscillator fits with real coupling to the low-frequency B_2 paraelectric spectra of the six arsenates at different temperatures.

	KDA					RbDA					CsDA					KD*A					RbD*A					CsD*A				
K	120	149	184	240	297	118	148	193	242	305	145	168	212	247	302	219	236	254	272	291	186	219	255	273	308	210	227	265	283	301
ω_a	97	108	117	128	147	117	128	140	159	171	146	148	156	157	163	82	93	95	97	104	100	111	115	115	117	86	90	94	105	108
ω_b	158	157	154	151	147	120	121	121	117	112	103	102	101	100	95	164	163	156	163	161	126	119	114	114	111	86	90	91	91	91
Γ_a	231	230	244	268	321	323	293	366	416	426	379	420	424	429	460	525	553	531	539	563	188	275	285	295	290	216	227	249	280	309
Γ_b	17	21	21	22	26	4	13	19	17	16	12	14	16	16	11	14	11	12	16	19	30	17	12	17	16	6	12	14	10	14
Δ	99	99	101	102	105	116	109	110	111	108	110	114	109	106	105	116	114	116	102	87	67	76	83	82	85	64	60	66	75	72

TABLE V. Values (in cm^{-1}) of ω_α, ω_β, Γ_α, Γ_β, and $\Gamma_{\alpha\beta}$ determined from the coupled-harmonic-oscillator fits with imaginary coupling to the low-frequency xy paraelectric spectra of the six arsenates at different temperatures.

	KDA					RbDA					CsDA					KD*A					RbD*A					CsD*A				
K	120	149	184	240	297	118	148	193	242	305	145	168	212	247	302	219	236	254	272	291	186	219	255	273	308	210	227	265	283	301
ω_α	69	88	94	95	98	27	61	69	76	81	30	46	59	62	62	51	69	73	80	82	13	19	31	32	35	11	15	21	25	29
ω_β	172	175	175	175	175	166	166	172	182	188	182	174	176	175	174	197	194	178	187	181	284	271	205	195	191	108	111	117	138	139
Γ_α	190	222	214	187	163	169	142	158	132	112	109	127	116	110	96	326	450	403	427	431	62	56	80	75	89	96	96	119	145	154
Γ_β	57	82	104	115	130	157	163	226	301	340	302	297	324	336	335	192	234	159	197	175	404	320	242	209	242	61	70	108	229	270
$\Gamma_{\alpha\beta}$	84	107	122	123	121	159	140	170	180	167	197	189	175	172	162	245	305	239	275	250	297	264	200	184	190	86	91	116	189	207

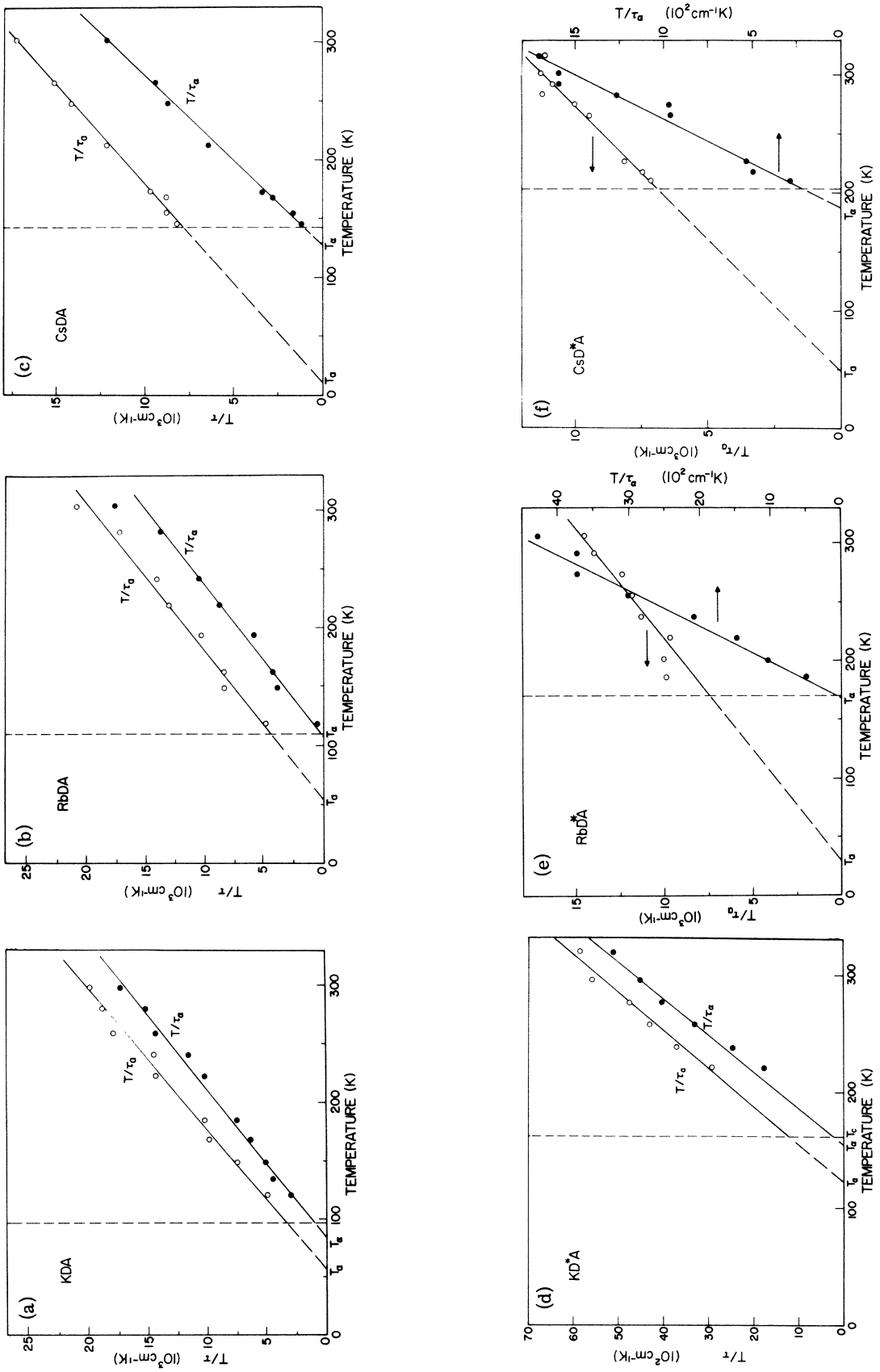

FIG. 5. Determined temperature dependence of T/τ_a and T/τ_α for (a) KDA, (b) RbDA, (c) CsDA, (d) KD*A, (e) RbD*A, and (f) CsD*A.

TABLE VI. Values of T_a and T_α, determined from the T/τ intercepts, $(T_c - T_A)/T_c = \delta/(K+\delta)$, and the individual proton or deuteron tunneling frequency Ω obtained as a solution of Eq. (9), using the listed values of T_a and the room-temperature values of ω_a given in Table IV.

	KDA	RbDA	CsDA	KD*A	RbD*A	CsD*A
T_c(K)	96	110	143	160	170	203
T_a(K)	60 ± 5	55 ± 9	10 ± 6	123 ± 13	29 ± 20	49 ± 7
Ω(cm^{-1})	99	125	115	74	71	69
T_α(K)	84 ± 5	108 ± 5	127 ± 3	155 ± 11	169 ± 5	187 ± 3
$\delta/(K+\delta)$	0.13	0.02	0.11	0.03	0.01	0.08

for the real coupling fit. In practice we have used such parameters as our starting estimates for the least-squares fits and this has sometimes led to slightly different final parameter values. It is these final parameters that are listed in Table V. The results reveal that mode α is a soft overdamped mode, while mode β is a comparatively weakly temperature-dependent (sometimes soft) mode which is heavily damped. The effects of deuteration do lead again to a significant decrease in the mode-α frequency; but mode β appears to be largely unaffected by a change in cation mass. Although the results are less physically appealing than for the case of real coupling, it is nevertheless clear that mode α describes the ferroelectric mode. In our following discussion of current theories of the hydrogen-bonded ferroelectrics it will be shown that one or other of the two forms of coupling will be the more appropriate form to be chosen.

As mentioned earlier, the standard deviations of the ω_i and Γ_i (for $i = a$ or α) parameters characterizing the ferroelectric mode were of the order of a few percent. Nevertheless, we have found that almost equivalent fits can be obtained for significantly different values of ω_i and Γ_i. As has been commented on elsewhere,[19] what does emerge from these fitting procedures is that the relaxation rate $1/\tau_i = \omega_i^2/\Gamma_i$ remains largely invariant to such different values of ω_i and Γ_i, and we accordingly put more emphasis on τ than the individual parameters when discussing the ferroelectric mode. Figure 5(a)–5(f) displays the educed temperature dependence of T/τ_a and T/τ_α for the six arsenates. Previous workers[19] have reported on the temperature dependence of T/τ_a for KDA and CsDA; although our results are in basic agreement with this previous work, they are not exactly so and we have therefore included our results to elucidate the later discussion.

It is apparent from Figs. 5(a)–5(f) that the T/τ determined for all the compounds vary linearly with temperature over the whole temperature range covered in these experiments. However, in no case do the T/τ vanish at the transition temperature[41]; the T/τ_a in fact extrapolate to zero significantly below the transition (as has been reported previously for KDA and CsDA[19]) while the T/τ_α go to zero within a few degrees of the transition temperature. Table VI summarizes the extrapolated values of the temperatures T_a and T_α at which T/τ_a and T/τ_α, respectively, vanish.

Two central features of importance emerge from these fitting analyses. First, the linear dependence on temperature of the T/τ found for all the compounds. Second, the failure of the T/τ values, for both real and imaginary coupling, to extrapolate to zero at the transition temperature. The linearity of T/τ with temperature might be expected, since in simplistic arguments both ω_i^2 and Γ_i should have a linear temperature dependence. However, the deviation of the T/τ from going to zero at the transition temperature may, at first, seem surprising. In making our fits to the coupled oscillator system, we have assumed the response function for both modes to have the form

$$G_i(\omega) = 2\omega_i^h/(\omega_i^2 - \omega^2 - i\omega\Gamma_i), \tag{4}$$

where ω_i^h is the truly harmonic frequency of the mode and ω_i contains the influence of the conventional real part of the anharmonic self-energy and Γ_i is a frequency-independent inverse lifetime. Because in a separate experiment [41] we have established that the static dielectric constant obeys Curie-Weiss behavior in the paraelectric phase of these materials, it follows from our assumed response functions that ω_i^2 should vary as

$$\omega_i^2 = K'(T - T_c), \tag{5}$$

with ω_i^2 becoming unstable at T_c. We now discuss the departure of our experimental data from this expected result and show that it is in accord with current theories of the hydrogen-bonded ferroelectrics.

In the Kobayashi model,[4] a collective proton-tunneling mode, of frequency Ω_p, is coupled electrostatically to a pure phonon of the same symmetry, of frequency ω_q. In the limit of small damping the coupled responses of the proton-phonon system can be written as

$$\omega_{\pm}^2 = \tfrac{1}{2}(\omega_q^2 + \Omega_p^2) \pm \{[\tfrac{1}{2}(\omega_q^2 - \Omega_p^2)]^2 + G^2\}^{1/2}, \quad (6)$$

where G^2 is an interaction term. It is readily shown that the ω_-^2 response has a temperature dependence varying as $(T - T_c)$ and is consequently identified as the ferroelectric mode; ω_+, on the other hand, is relatively temperature independent. Kobayashi's theory was formulated within the approximation assuming only one proton per unit cell coupling with a single phonon. In reality, of course, there are four protons per unit cell and a more appropriate calculation,[42] which takes into account all four protonic interactions, yields four collective modes with frequencies (and their symmetries) of ω_1 (B_2), ω_2 and ω_3 (E) and ω_4 (A_2) such that

$$\omega_1 < \omega_2 = \omega_3 < \omega_4 . \quad (7)$$

It is found that, of these modes, only ω_1 is strongly temperature dependent and is therefore associated with ω_-.

In the absence of the lattice coupling, the collective tunneling frequency is given by[4,43]

$$\Omega_p^2 = 4\Omega^2 - \Omega J \tanh(\Omega/kT), \quad (8)$$

where Ω is the individual proton tunneling frequency and J is the dipolar proton-proton interaction. The collective tunneling frequency has a soft-mode temperature dependence[2,3] which leads to a transition at a temperature T_0 such that $T_0 < T_c$. If $\Omega_p^2 = 0$ at $T = T_0$, then it is readily shown that

$$\Omega_p^2 = 4\Omega^2\left[1 - \tanh\left(\frac{\Omega}{kT}\right)\Big/ \tanh\left(\frac{\Omega}{kT_0}\right)\right]. \quad (9)$$

Within the same limit of small damping, the coupled oscillator system with real coupling (this form of coupling is the more appropriate in view of the nondissipative nature of the Kobayashi theory) discussed earlier has coupled responses of the form

$$\omega_{\pm}^2 = \tfrac{1}{2}(\omega_b^2 + \omega_a^2) \pm \{[\tfrac{1}{2}(\omega_b^2 - \omega_a^2)]^2 + \Delta^4\}^{1/2}. \quad (10)$$

Within this approximation, therefore, the behavior of the coupled-harmonic-oscillator system, described by Eq. (10), is formally equivalent to that of the Kobayashi system, described by Eq. (6), with ω_a analogous to Ω_p and ω_b analogous to ω_q.[27] As mentioned above, the collective tunneling frequency is a soft mode which becomes unstable at a temperature below T_c and such behavior is observed for ω_a as discussed earlier. Formally, therefore, the values in Tables IV and VI of ω_a and T_a determine the values of Ω_p and T_0 for the different materials. The use of these values then leads to a solution of Eq. (9) for the individual proton tunneling frequency Ω. Values of Ω determined at close to room temperature are listed in Table VI. The significant outcome of these calculations is that, as would be expected, the individual deuteron tunneling frequency is small compared to that for the proton in the corresponding hydrogenated compounds. It is worth noting here that previous attempts[4] to determine Ω have involved the assumption that the term G^2 [see Eq. (6)] is small compared to $[\frac{1}{2}(\Omega_p^2 - \omega_q^2)]^2$, whereas inspection of Table IV shows that, by analogy to the equivalent coupled-harmonic-oscillator parameters, the reverse is true. However, a persuance of this train of thought stemming from the formal equivalence of the coupled-harmonic-oscillator and Kobayashi model should be undertaken with caution in view of the unrealistic approximation assumed of small damping. Furthermore, as Fig. 6 shows for CsDA and CsD*A, although our calculations of ω_-^2 from Eq. (10) do reveal ω_- to represent a soft mode, in no case do the results lead to a $(T - T_c)$ temperature dependence with ω_-^2 going to zero at T_c. When damping is included, of course, the actual coupled responses of the oscillator system are given by solutions of the equation

$$\omega^4 - i\omega^3(\Gamma_a + \Gamma_b) - \omega^2(\omega_a^2 + \omega_b^2 + \Gamma_a\Gamma_b) + i\omega(\omega_a^2\Gamma_b + \omega_b^2\Gamma_a) + \omega_a^2\omega_b^2 - \Delta^4 = 0. \quad (11)$$

Table VII compares values of ω_+ and ω_- determined from Eqs. (10) and (11) and the large deviations between the two sets of values emphasize the importance of the large damping in determining the actual coupled responses of the system and cast doubts on the ability of the Kobayashi model to seriously describe the hydrogen-bonded ferroelectric transition.

The limit of small damping is but one weakness of the Kobayashi model,[8-10] and a number of authors have recently attempted to describe the ferroelectric transition in terms of anharmonic pho-

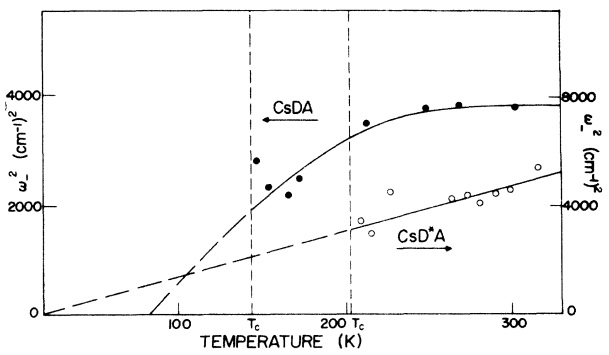

FIG. 6. Temperature dependence of ω_-^2 determined from Eq. (10) for CsDA and CsD*A.

TABLE VII. Comparison of values of ω_+ and ω_- obtained as solutions to Eqs. (10) and (11).

	T	From Eq. (10) ω_+	From Eq. (10) ω_-	From Eq. (11) ω_+	From Eq. (11) ω_-
KDA	297	180	103	148	0
RbDA	305	188	81	110	0
CsDA	302	178	61	92	0
KD*A	291	170	88	161	0
RbD*A	308	143	76	112	0
CsD*A	301	123	67	90	0

nons.[13-16] In recent papers Cowley and Coombs[15,16] have shown that, for piezoelectric crystals at low frequencies, there is an additional contribution to the self-energy of the ferroelectric mode which decreases the real part of the self-energy and increases the damping. This additional contribution arises from the deviations introduced into the phonon distribution by the fluctuations of the ferroelectric mode of the piezoelectric system and leads to a response function for the ferroelectric mode of

$$G_i(\omega) = 2\omega_i^h/(\omega_i^2 - \omega^2 - i\omega\Gamma_i - H)\,, \tag{12}$$

where

$$H = 72\omega_i^h \sum \left| V\begin{pmatrix} 0 & q_1 & -q_1 \\ t & j_1 & j_1 \end{pmatrix}\right|^2 \times [n_1(n_1+1)\,\beta\hbar^{-1}] \times \left(1 - \frac{\omega}{\omega + i/\tau_1}\right), \tag{13}$$

where the V are Fourier transforms of the second-order cubic coefficients in the Taylor expansion of the potential energy. If we assume the lifetime τ_1 of all the other phonons is the same, τ, then in the high-temperature limit the Green's function becomes

$$G_i(\omega) = \frac{2\omega_i^h}{\omega_i^2 - \omega^2 - i\omega\Gamma_i - \delta T/(1+i\omega\tau)}, \tag{14}$$

where δ is a positive constant. At high frequencies, where $\omega\tau \gg 1$, the response function reduces to a damped-harmonic-oscillator form with a frequency ω such that

$$\omega_i^2 = (K+\delta)(T - T_A)\,, \tag{15}$$

while at low frequencies, where $\omega\tau \ll 1$, the response function reduces to a damped-oscillator form with a frequency Ω_1 such that

$$\Omega_i^2 = \omega_i^2 - \delta T = K(T - T_c)\,, \tag{16}$$

where

$$\delta/(K+\delta) = 1 - T_A/T_c\,. \tag{17}$$

Equation (17) reveals that the ferroelectric mode will vanish below T_c at a temperature T_A. In drawing comparisons between the ω_i in Eq. (15) and the results of our coupled oscillator fits it is important to note that ω_α, and not ω_a, is the more appropriate value to be used. That this is true can be seen from Eqs. (10) and (11), from which it can be shown that ω_a will not be identically zero when ω_- vanishes at the ferroelectric transition temperature. For real coupling, therefore, ω_a will go to zero below T_c even if $\delta = 0$. For imaginary coupling, however, the coupled responses of the double-oscillator system are solutions of

$$\omega^4 - i\omega^3(\Gamma_\alpha + \Gamma_\beta) - \omega^2(\omega_\alpha^2 + \omega_\beta^2 + \Gamma_\alpha\Gamma_\beta - \Gamma_{\alpha\beta}^2) + i\omega(\omega_\alpha^2\Gamma_\beta + \omega_\beta^2\Gamma_\alpha) + \omega_\alpha^2\,\omega_\beta^2 = 0 \tag{18}$$

and it can be shown that one solution exists when ω_- and ω_α (or ω_β) are identically zero. For imaginary coupling, therefore, any deviation from ω_α^2 vanishing at T_c can be ascribed to the anomalous self-energy term δ, with T_α being analogous to T_A. The values of T_α given in Table VI support the claim of Eq. (17) that $T_A \equiv T_\alpha < T_c$. It follows that the ratio $(T_c - T_A)/T_c$ determines an estimate of the ratio of the anomalous contribution to the self-energy to that of the regular term for the ferroelectric mode for $\omega = 0$. Values of such ratios are listed in Table VI from which it appears that the anomalous self-energy is small compared to the conventional anharmonic self-energy of the soft mode. No significant trends emerge from this data, although it appears that the $\delta/(K+\delta)$ ratios are always larger for the hydrogenated compounds than for the corresponding deuterated compounds, and that the $\delta/(K+\delta)$ ratios for the rubidium compounds are very small.

IV. CONCLUSIONS

Through examination of the molecular Raman spectra for the KDA isomorphs, hydrogenated and deuterated, we have identified the protonic (deuteronic), transverse optic, AsO_4^{3-} internal, and O–H–O valence vibration contributions to the Raman scattering and determined their symmetries, mass, and temperature dependence. The transverse-optic-mode frequencies agree reasonably well with those calculated by Shur for KDP.[32] The internal arsenate modes correspond well in frequency to those observed in solution and other compounds,[35] and are observed to be split predominantly by their S_4 site symmetry in the KDA lattice. The O–H–O vibrations exist as very broad bands in the region 1000–3000 cm^{-1} and are seen to lower in frequency by a factor of ~0.73 upon substitution of deuterium for hydrogen. These bands continue to exist in similar form in the ferroelectric phase. The marked breadth of many spectral features is seen to disappear in the ferroelectric phase, sug-

gesting that it is related to the disorder of the protons (deuterons) above the transition.

Evidence for the collective protonic or deuteronic motions is observed in both the low-frequency B_2 and E spectra in the paraelectric phase and the following conclusions emerge. First, the complexity of the E spectra in all cases precludes a detailed examination of the contributing modes in terms of just two interacting oscillators. Secondly, the low-frequency B_2 spectra for the hydrogenated compounds are well fitted by a coupled-oscillator system representing the ferroelectric mode and a low-frequency phonon. Third, the low-frequency B_2 spectra for the deuterated compounds appear to imply that the ferroelectric mode is coupled to at least two low-frequency phonons, and that a two-coupled-oscillator system can at best only be used as an approximation to describe these spectra. Fourth, the T/τ for all the compounds are well determined and vary linearly with temperature with T/τ_a extrapolating to zero well below the transition temperature and T/τ_α going to zero much closer to the transition temperature. Fifth, the choice of real coupling between the two oscillators is the more appropriate in drawing analogies with the Kobayashi theory but although the results, in the limit of small damping, support the soft-mode behavior of the collective proton-tunneling mode, they do not lead to ω_-^2 varying as $(T - T_c)$; in the presence of damping, however, the actual ω_-^2 values are shown to be significantly different from the values determined in the limit of small damping. Sixth, the choice of imaginary coupling is more appropriate in discussing the anharmonic theories of Cowley and Coombs and reveal the anomalous self-energy to be small compared to the conventional real anharmonic self-energy of the ferroelectric mode.

ACKNOWLEDGMENTS

We are pleased to acknowledge helpful discussions with Professor J. S. Scott and Professor C. Y. She and we would like to thank Dr. G. A. Samara for a preprint of his work with Dr. P. S. Peercy on RbH_2PO_4. We are also indebted to Professor D. Bowen of this Physics Department for aid in implementing the curve-fitting techniques.

---

*Work supported by a grant from the Army Research Office, Durham, N. C. Part of the equipment used in this work was provided under NASA Cooperative Agreement NCAw 22-011-079.

[1]P. A. de Gennes, Solid State Commun. 1, 132 (1963).
[2]R. Brout, K. A. Müller, and H. Thomas, Solid State Commun. 4, 507 (1966).
[3]M. Tokunaga, Prog. Theor. Phys. 36, 857 (1966).
[4]K. Kobayashi, J. Phys. Soc. Jap. 24, 497 (1968).
[5]V. Dvořák, Czech. J. Phys. B 20, 1 (1970).
[6]E. M. Brody and H. Z. Cummins, Phys. Rev. Lett. 21, 1263 (1968).
[7]E. M. Brody and H. Z. Cummins, Phys. Rev. Lett. 23, 1039 (1969).
[8]R. Blinc, V. Dimic, J. Petkovsek, and E. Pirkmajer, Phys. Lett. A 26, 8 (1967).
[9]T. Fujiwara, J. Phys. Soc. Jap. 29, 1282 (1970).
[10]R. L. Reese, I. J. Fritz, and H. Z. Cummins, Phys. Rev. B 7, 4165 (1973).
[11]R. Blinc, J. Phys. Chem. Solids 13, 204 (1960).
[12]R. Blinc and M. Ribaric, Phys. Rev. 130, 1816 (1963).
[13]R. A. Cowley, J. Phys. Soc. Jap. Suppl. 28, 239 (1970).
[14]M. A. Moore and H. C. W. L. Williams, J. Phys. C 5, 3168 (1972); 5, 3185 (1972); 5, 3222 (1972).
[15]G. J. Coombs and R. A. Cowley, J. Phys. C 6, 121 (1973).
[16]R. A. Cowley and G. J. Coombs, J. Phys. C 6, 143 (1973).
[17]D. K. Agrawal and C. H. Perry, *Proceedings of the Second International Conference on Light Scattering in Solids*, edited by M. Balkanski (Flammarion, Paris, 1971), p. 429.
[18]H. Hammer, *Proceedings of the Second International Conference on Light Scattering in Solids*, edited by M. Balkanski (Flammarion, Paris, 1972), p. 425.
[19]R. S. Katiyar, J. F. Ryan, and J. F. Scott, *Proceedings of the Second International Conference on Light Scattering in Solids*, edited by M. Balkanski (Flammarion, Paris, 1971), p. 436; Phys. Rev. B 4, 2635 (1971).
[20]R. C. Leung, R. P. Lowndes, and N. E. Tornberg, Phys. Lett. A 44, 383 (1973).
[21]Landolt-Börnstein, *Ferroelectric and Antiferroelectric Substances* (Springer-Verlag, Berlin, 1969) Vol. 3, p. 141.
[22]M. S. Shur, Kristallografiya 11, 448 (1965)[Sov. Phys.-Crystallogr. 11, 394 (1966)].
[23]J. C. Slater, J. Chem. Phys. 9, 16 (1941).
[24]I. P. Kaminow, Phys. Rev. A 138, 1539 (1965).
[25]I. P. Kaminow and T. C. Damen, Phys. Rev. Lett. 20, 1105 (1968).
[26]C. Y. She, T. W. Broberg, L. S. Wall, and D. F. Edwards, Phys. Rev. B 6, 1847 (1972).
[27]P. S. Peercy and G. A. Samara, Phys. Rev. B 8, 2033 (1973).
[28]B. Lavrenčič, I. Levstek, B. Žekš, R. Blinc, and D. Hadži, Chem. Phys. Lett. 5, 441 (1970).
[29]J. F. Scott and C. M. Wilson, Solid State Commun. 10, 597 (1972).
[30]T. W. Broberg, C. Y. She, L. S. Wall, and D. F. Edwards, Phys. Rev. B 6, 3332 (1972).
[31]M. S. Shur, Kristallografiya 12, 215 (1967)[Sov. Phys.-Crystallogr. 12, 181 (1967)].
[32]M. S. Shur, Fiz. Tverd. Tela 8, 57 (1966)[Sov. Phys.-Solid State 8, 43 (1966)].
[33]A. I. Stekhanov and E. A. Popova, Fiz. Tverd. Tela 7, 3530 (1965) [Sov. Phys.-Solid State 7, 2849 (1966)].
[34]C. Y. She, T. W. Broberg, and D. F. Edwards, Phys. Rev. B 4, 1580 (1971).
[35]F. Fehér and G. Morgenstern, Z. Anorg. Allg. Chem. 232, 169 (1937).
[36]G. Herzberg, in *Molecular Spectra and Molecular Struc-*

ture (Van Nostrand, Princeton, N. J., 1964), Vol. II.
[37]I. P. Kaminow, R. C. C. Leite, and S. P. S. Porto, J. Phys. Chem. Solids 26, 2085 (1965).
[38]E. V. Chisler, I. T. Savatinova, and V. Yu Davydov, Fiz. Tverd. Tela 13, 1599 (1971)[Sov. Phys.-Solid State 13, 1339 (1971)].
[39]E. V. Chisler, V. Yu Davydov, and I. T. Savatinova, Fiz. Tverd. Tela 13, 1949 (1971)[Sov. Phys.-Solid State 13, 1635 (1972)].
[40]A. S. Barker and J. J. Hopfield, Phys. Rev. 135, 1732 (1964).
[41]R. P. Lowndes and W. B. Spillman (unpublished).
[42]R. Brout, K. A. Müller, and H. Thomas, Solid State Commun. 4, 1105 (1967).
[43]W. Cochran, Adv. Phys. 18, 157 (1969).